Original Article

OPEN

# Signal Transducer and Activator of Transcription 3/MicroRNA-21 Feedback Loop Contributes to Atrial Fibrillation by Promoting Atrial Fibrosis in a Rat Sterile Pericarditis Model

Zhengrong Huang, MD, PhD*; Xiao-jun Chen, MD*; Cheng Qian, MD*; Qian Dong, MD, PhD; Dan Ding, MD; Qiong-feng Wu, MD; Jing Li, MD; Hong-fei Wang, MD, PhD; Wei-hua Li, MD, PhD; Qiang Xie, MD, PhD; Xiang Cheng, MD, PhD; Ning Zhao MD, PhD; Yi-mei Du, MD, PhD; Yu-hua Liao, MD

***Background***—Postoperative atrial fibrillation is a frequent complication in cardiac surgery. The aberrant activation of signal transducer and activator of transcription 3 (STAT3) contributes to the pathogenesis of atrial fibrillation. MicroRNA-21 (miR-21) promotes atrial fibrosis. Recent studies support the existence of reciprocal regulation between STAT3 and miR-21. Here, we test the hypothesis that these 2 molecules might form a feedback loop that contributes to postoperative atrial fibrillation by promoting atrial fibrosis.

***Methods and Results***—A sterile pericarditis model was created using atrial surfaces dusted with sterile talcum powder in rats. The inflammatory cytokines interleukin (IL)-1β, IL-6, transforming growth factor-β, and tumor necrosis factor-α, along with STAT3 and miR-21, were highly upregulated in sterile pericarditis rats. The inhibition of STAT3 by S3I-201 resulted in miR-21 downregulation, which ameliorated atrial fibrosis and decreased the expression of the fibrosis-related genes, α-smooth muscle actin, collagen-1, and collagen-3; reduced the inhomogeneity of atrial conduction; and attenuated atrial fibrillation vulnerability. Meanwhile, treatment with antagomir-21 decreased STAT3 phosphorylation, alleviated atrial remodeling, abrogated sterile pericarditis–induced inhomogeneous conduction, and prevented atrial fibrillation promotion. The culturing of cardiac fibroblasts with IL-6 resulted in progressively augmented STAT3 phosphorylation and miR-21 levels. S3I-201 blocked IL-6 induced the expression of miR-21 and fibrosis-related genes in addition to cardiac fibroblast proliferation. Transfected antagomir-21 decreased the IL-6–induced cardiac fibroblast activation and STAT3 phosphorylation. The overexpression of miR-21 in cardiac fibroblasts caused the upregulation of STAT3 phosphorylation, enhanced fibrosis-related genes, and increased cell numbers.

***Conclusions***—Our results have uncovered a novel reciprocal loop between STAT3 and miR-21 that is activated after heart surgery and can contribute to atrial fibrillation. **(*Circ Arrhythm Electrophysiol*. 2016;9:e003396. DOI: 10.1161/CIRCEP.115.003396.)**

**Key Words:** arrhythmia ■ atrial fibrillation ■ microRNA ■ signal transduction

Atrial fibrillation (AF) is the most common sustained arrhythmia in clinical practice and is a well-known complication after cardiac surgery. The incidence of postoperative AF (POAF) varies between 10% and 60%. POAF is associated with an increased risk of congestive heart failure, renal insufficiency, and stroke, all of which prolong hospital stays and increase expenses after heart surgery.[1] In many clinical studies, higher levels of inflammatory markers (such as C-reactive protein and interleukin [IL]-6) and elevated white blood cell counts have been reported to be associated with POAF.[2,3] The role of inflammation in POAF has been further confirmed in canine sterile pericarditis (SP), an experimental model of POAF in humans.[4] This model is characterized by the atrial infiltration of neutrophils, significant fibrosis, and increased levels of C-reactive protein and IL-6.[5,6] Indeed, elevated IL-6 induces cardiac fibrosis, myocardial hypertrophy,[7,8] and AF.[9,10]

Received July 23, 2015; accepted June 6, 2016.

For the author affilations, please see the Appendix.

*Drs Huang, Chen, and Qian contributed equally to this work.

**The Data Supplement is available at http://circep.ahajournals.org/lookup/suppl/doi:10.1161/CIRCEP.115.003396/-/DC1.**

Correspondence to Yi-Mei Du, MD, PhD, Research Center of Ion Channelopathy, Institute of Cardiology, Union Hospital, Tongji Medical College, Huazhong Univ of Science and Technology, Jiefang Ave 1277, Wuhan, Hubei, 430022, P. R. China, E-mail yimeidu@mail.hust.edu.cn or Ning Zhao MD, PhD, Research Center of Ion Channelopathy, Institute of Cardiology, Union Hospital, Tongji Medical College, Huazhong Univ of Science and Technology, Jiefang Ave 1277, Wuhan, Hubei, 430022, P. R. China, E-mail zhaoning19870403@126.com

### WHAT IS KNOWN

- The aberrant activation of STAT3 and the increased expression of miR-21 contribute to fibrotic processes linked to AF.
- The reciprocal regulation between STAT3 and miR-21 has been demonstrated in malignant disease.

### WHAT THE STUDY ADDS

- The inhibition of STAT3 or miR-21 ameliorated atrial fibrosis and prevented inducible AF in SP rats.
- A novel reciprocal loop between STAT3 and miR-21 that is activated after heart surgery can contribute to AF by promoting atrial fibrosis.

However, the exact molecular mechanism of POAF remains incompletely understood.[11]

Signal transducer and activator of transcription 3 (STAT3) is an important transcription factor that regulates many biological processes.[12] Its activation by cytokines and growth factors induces STAT3 tyrosine-705 phosphorylation and cytoplasmic-to-nuclear shuttling, the recognition of STAT3-specific DNA-binding elements, and the transcriptional activation of its target genes.[13,14] Aberrant STAT3 activation often occurs after IL-6 stimulation, which is involved in the pathogenesis of various cardiovascular diseases.[13,14] Recently, the activation of STAT3 by IL-6 was found to promote cell proliferation and differentiation and the synthesis of collagens in cardiac fibroblasts (CFs).[13,15] Furthermore, increased STAT3 activation has been reported in response to inflammatory changes and atrial fibrosis both in AF animal models[16] and in patients.[17] Moreover, the inhibition of STAT3 by S3I-201, a novel selective inhibitor of STAT3,[18] significantly suppressed the expression of α-smooth muscle actin (α-SMA), decreased IL-6–induced collagen synthesis, and effectively reduced the fibrosis process.[19] Therefore, the activation of STAT3 might contribute to the pathophysiology of POAF.

MicroRNAs (miR) are a class of small noncoding RNAs that repress gene expression at the post-transcriptional level by targeting mRNA. Accumulating evidence implicates miR-21 in a variety of disorders and indicates that it is highly upregulated during cardiac fibrosis.[20–23] The expression of miR-21 is also increased in atrial tissues[24,25] and plasma samples from patients with AF.[26] Importantly, atrial miR-21 knockdown with antagomir-21 suppresses atrial fibrosis and reduces AF promotion in rats after chronic myocardial infarction,[27] making this molecule an effective target for AF treatment. Recent studies have demonstrated that STAT3 can regulate miR-21 expression[28–30]; moreover, miR-21 also modulates the STAT3 signaling pathway.[31–33] In addition, given the importance of both STAT3 and miR-21 in the fibrotic processes linked to AF, we hypothesized that they might form a reciprocal positive loop that contributes to POAF by promoting atrial fibrosis.

In this study, we first assessed the changes in atrial profibrillatory remodeling and inflammatory cytokines with the expression of STAT3 and miR-21 in the rat model of SP. We then explored the anti-AF effects of S3I-201 and antagomir-21 in the same model. In addition, the interaction between STAT3 and miR-21 was investigated in cultured CFs to elaborate on their roles in atrial fibrosis. Our data reveal, for the first time, that the STAT3/miR-21 positive feedback loop might contribute to AF by promoting atrial fibrosis in SP rats.

## Materials and Methods

For additional details, please see Materials and Methods section in the Data Supplement.

### Preparation of the SP

A total of 176 adult male Sprague-Dawley rats weighing 180 to 220 g were purchased from the Animal Center, Tongji Medical College, Huazhong University of Science and Technology, Wuhan, China. The study was approved by the Animal Research Ethics Committee of Tongji Medical College, Huazhong University of Science and Technology, in compliance with the National Institutes of Health Guide for the Care and Use of Laboratory Animals (NIH Publication, revised 2011).

The SP model was induced as described in our previous study.[34] Briefly, rats were anesthetized by intraperitoneal injection of sodium pentobarbital (40 mg/kg), intubated, and ventilated. The chest skin was shaved and sterilized with 75% alcohol. The heart was exposed through the left second intercostal space. After a pericardiotomy, the atrial surfaces were generously dusted with sterile talcum powder and then covered by a single layer of gauze. Sham-operated animals were subjected to the same procedure without pericardiotomy.

### In Vivo Electrophysiology

In vivo electrophysiology was performed as previously described.[34] Briefly, a 6F 10 pole coronary sinus electrode catheter (ten 0.5-mm circular electrodes; interelectrode distance 2.0 mm; and electrode pair spacing 6.0 mm) was inserted into the esophagus for recording and stimulation. The ECG was continuously monitored. To induce AF, 5 consecutive 30-second bursts of rapid stimulation (25, 30, 40, 50, and 83 Hz) were performed at 3-minute intervals. AF was defined as rapid and fragmented atrial electrograms with irregular atrioventricular nodal conduction and ventricular rhythm for at least 2 seconds. The AF duration was measured until the ECG showed a sinus rhythm again. The total time of the AF episodes was defined as the sum of the AF duration of each episode. The probability of induction of AF was determined by calculating the number of AF episodes divided by the number of total procedures.

### Epicardial Activation Mapping

Atrial epicardial activation mapping in isolated Langendorff-perfused hearts was performed using a multielectrode array containing 32 electrodes (Figure IA and IB in the Data Supplement; 0.2-mm electrode diameter; 0.36-mm interelectrode distance).[35] Activation times were determined as the point of maximal negative slope and displayed in a grid representing the layout of the original recording array (Figure IC in the Data Supplement). All activation times were related to the timing of the first detected waveform and then used to draw activation maps in MATLAB. The maximal vectorial conduction velocity and the index of inhomogeneity were calculated as previously described.[36,37]

### Experimental Protocols In Vivo

To examine the role of STAT3/miR-21 in postoperative AF in SP rats, the STAT3 inhibitor S3I-201 (5 mg/kg, dissolved in 50 μL dimethyl sulfoxide, Selleck) was administered intraperitoneally once daily for 3 days, and 5 μL antagomir-21 (7.5 nmol, Ribobio, Guangzhou, China) was injected with a Hamilton microsyringe (33-gauge needle) into the left atrial wall at 5 separate injection points immediately after the pericardiotomy. Control rats were injected with the same volume of the vehicle.

## CF Isolation

Primary cultures of rat CFs were isolated from the hearts of 1- to 2-day-old (neonatal) Sprague-Dawley rats or the atria of 8- to 14-week-old (adult) Sprague-Dawley rats using an enzymatic digestion solution containing 0.1% collagenase (type II, Worthington Biochemical, NJ) and 0.25% trypsin (Amresco, Cleveland, OH) at 37 °C. The second- or third-generation CFs were used in all subsequent experiments.

## Cell Treatments

Cells were incubated with 20 ng/mL recombinant rat IL-6 (Pepro Tech, Rocky Hill, NJ) for the indicated time periods. To elucidate the role of miR-21 in cardiac fibrosis, we transfected synthesized miR-21 mimics (5′-UAGCUUAUCAGACUGAUGUUGA-3′ or antagomir-21 (5′-UCAACAUCAGUCUGAUAAGCUA-3′; Ribobio) into CFs using ribo FECT CP (Ribobio) according to the manufacturer's protocol. Control oligonucleotides (Ribobio) were transfected into the negative control samples. Twenty-four hours after transfection, the transfected cells were incubated with IL-6 (20 ng/mL) or S3I-201 (50 μmol/L) for another 24 hours.

## Western Blot Analysis

Total protein samples were extracted from tissues or whole cells by the standard procedure. Samples (20 μg) were run on a 10% SDS-PAGE gel followed by blotting to a nitrocellulose membrane. After blocking, the membranes were probed with anti-Tyr$^{705}$ phosphorate STAT3 (P-STAT3) or total STAT3 (T-STAT3; diluted 1:1000; Cell Signaling Technology) overnight at 4°C. The band intensity was assessed using the Image Lab software (Bio-Rad, Richmond, CA) and referenced to GAPDH (diluted 1:500; Aspen, Wuhan, China).

## Real-Time Polymerase Chain Reaction

Real-time polymerase chain reaction (PCR) was performed as previously described[38] using gene-specific primer pairs (Table I in the Data Supplement).

## Atrial Histology and Immunohistochemical Staining

Tissue samples from the atria were fixed with 4% paraformaldehyde, embedded in paraffin, and sliced into 4-μm-thick sections, which were stained with hematoxylin–eosin and Masson trichrome.

A separate group of sections was immunostained with primary antibodies against rat P-STAT3 (diluted 1:50; Cell Signaling Technology) and α-SMA (diluted 1:50, Boster, Wuhan, China), followed by incubation with biotin-conjugated secondary antibodies, then treated with avidin–peroxidase. The reaction was developed using the DAB substrate kit (BioSci, Wuhan, China), and the sections were counterstained with hematoxylin–eosin.

## Determination of Cell Proliferation

Cell proliferation was measured using the Cell Counting Kit-8 (CCK-8; Dojindo Molecular Technologies, Tokyo, Japan).

## Statistical Analysis

Results are reported as the mean±SEM. An unpaired *t* test or Welch *t* test was used for 2-group comparisons. Group comparisons were conducted by analysis of variance using Tukey post-test. Statistical analyses were performed using SPSS version 18.0, and $P<0.05$ was considered statistically significant.

# Results

## Characterization of the Model

The basic ECG parameters and the cardiac electrophysiology data are presented in Table 1. No significant differences were observed in the parameters examined. Typical ECG recordings before and after transesophageal burst pacing are presented in Figure 1A and 1B. The analysis results for the total AF duration and the probability of induction of AF at day 3 after surgery are depicted in Figure 1C and 1D. Similarly to our previous report,[34] the total AF duration was significantly longer and the probability of AF significantly higher in the SP rats (n=10) than in the sham

**Table. Evaluation of Surface ECG Parameters, Transesophageal Recording, and Atrial Epicardial Activation Mapping**

| | Control | Sham | SP | S3I-201 | Antagomir-21 |
|---|---|---|---|---|---|
| RR, ms | 135±3.36 | 137±3.43 | 137±2.86 | 137.43±2.66 | 136.67±2.36 |
| P, ms | 19.93±0.73 | 20.83±0.83 | 21±0.37 | 20.6±0.31 | 20.33±0.42 |
| PR, ms | 46.33±1.44 | 46.83±1.45 | 46.83±1.45 | 46.13±1.94 | 46.33±2.14 |
| QRS, ms | 19±0.52 | 19.5±0.72 | 19.33±0.61 | 19.13±0.87 | 19.23±0.92 |
| QT, ms | 78.67±1.97 | 79.33±2.17 | 77±2.44 | 78.47±2.83 | 77.34±2.94 |
| CSNRT, ms | 38±2.59 | 38.5±2.63 | 43.83±4.92 | 41.13±5.12 | 41.33±5.22 |
| WCL, ms | 87.07±1.71 | 87.67±1.91 | 88.33±1.69 | 87.33±1.99 | 87.33±1.89 |
| AVERP120, ms | 69.33±2.28 | 70±2.78 | 71.33±0.99 | 71.13±1.20 | 70.93±1.34 |
| AVERP110, ms | 70.67±2.27 | 71±2.67 | 72±1.03 | 71.33±2.33 | 71.16±1.63 |
| AVERP100, ms | 71.33±2.27 | 72±2.97 | 73.33±1.33 | 72.13±1.96 | 72.63±1.93 |
| CV, mm/ms | 0.45±0.01 | 0.51±0.03 | 0.56±0.04 | 0.41±0.10 | 0.43±0.01 |
| Index | 1.26±0.10 | 1.17±0.10 | 2.66±0.20* | 2.03±0.13† | 1.25±0.15‡ |

ECG and transesophageal recording from control (n=8), sham (n=10), and SP rats (n=10), S3I-301 (n=5) and Antagomir-21 (n=5). Epicardial activation mapping from control (n=6), sham (n=9), and SP rats (n=11), S3I-301 (n=6) and Antagomir-21 (n=4). AVERP indicates atrioventricular nodal refractory period; CSNRT, corrected sinus node recovery time; CV, conductive velocity; Index, inhomogeneity index; Sham, sham-operated rats; SP, rats with sterile pericarditis; and WCL, Wenckebach cycle length.

*$P<0.001$ vs sham.

†$P<0.05$.

‡$P<0.01$ vs SP.

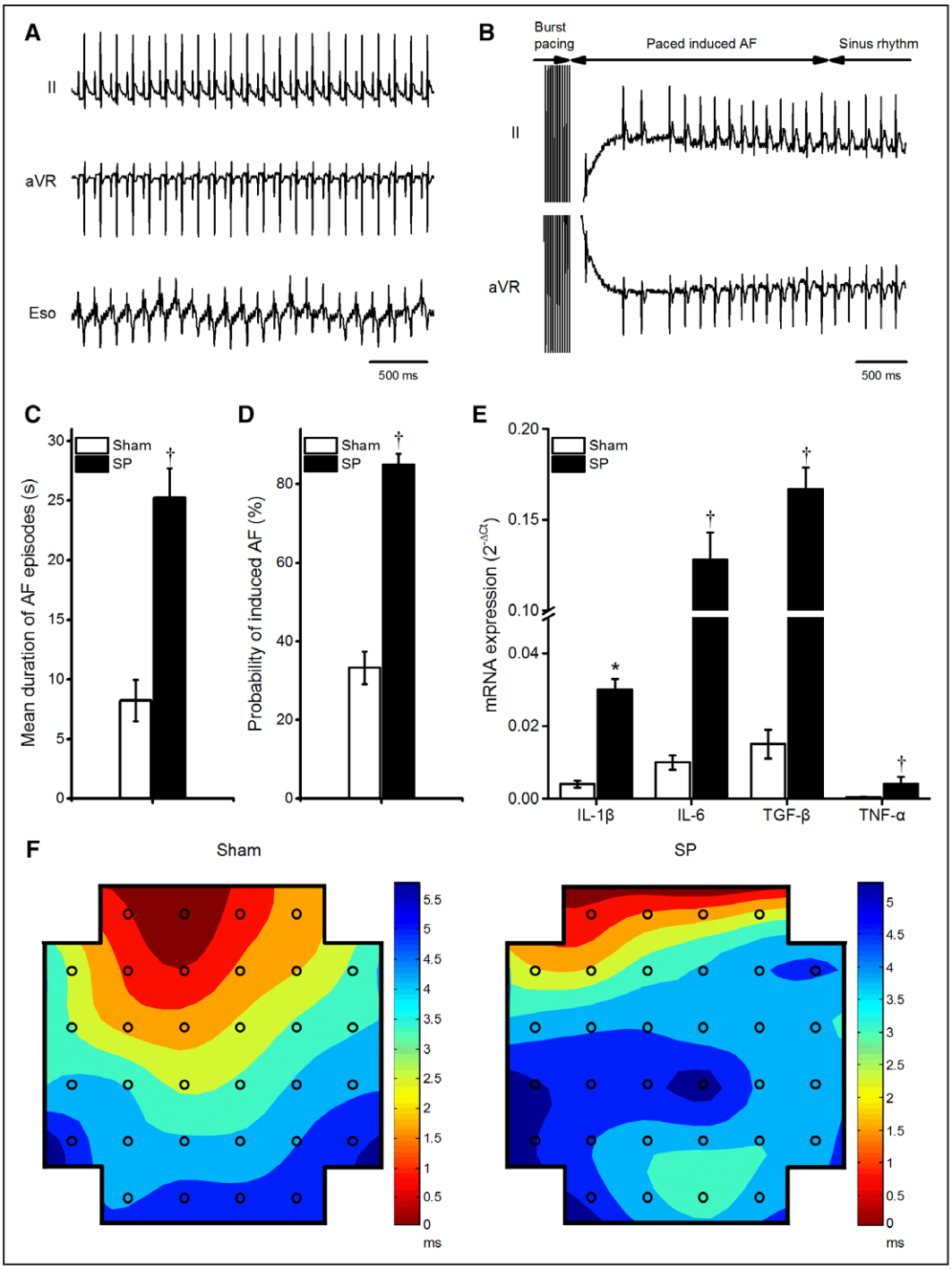


**Figure 1.** A typical tracing of ECG and esophageal electrogram during sinus rhythm (**A**). A typical time course of induced atrial fibrillation (AF) followed by burst pacing (**B**). ECG showing induced AF after burst pacing and spontaneous AF termination. Mean duration of AF episodes (**C**) and probability of induced AF (**D**). The mRNA levels of AF-related proinflammatory cytokines interleukin (IL)-1β, IL-6, transforming growth factor (TGF)-β and tumor necrosis factor (TNF)-α in the atria (**E**). **P*<0.01, †*P*<0.001 vs sham. Representative examples of spontaneous conduction properties of epicardial activation mapping in sham (**left**) and sterile pericarditis (SP; **right**) rats analyzed by multielectrode array (**F**). aVR indicates rightarm augmented unipolar lead; and Eso, esophagus.

rats (n=10). Real-time PCR showed that the expression of proinflammatory cytokines IL-1β, IL-6, transforming growth factor-β, and tumor necrosis factor-α was highly upregulated in the SP rats compared with the sham rats (Figure 1E). To evaluate the atrial conduction properties, we performed epicardial multielectrode array mapping in isolated Langendorff-perfused hearts. Figure 1F and Figure IC in the Data Supplement show representative examples of right atrium activation during sinus rhythm from a sham rat (left) and a SP rat on postoperative day 3 (right). In contrast to the atrial activation patterns in sham rats, the maps from SP rats were characterized by inhomogeneous conduction.

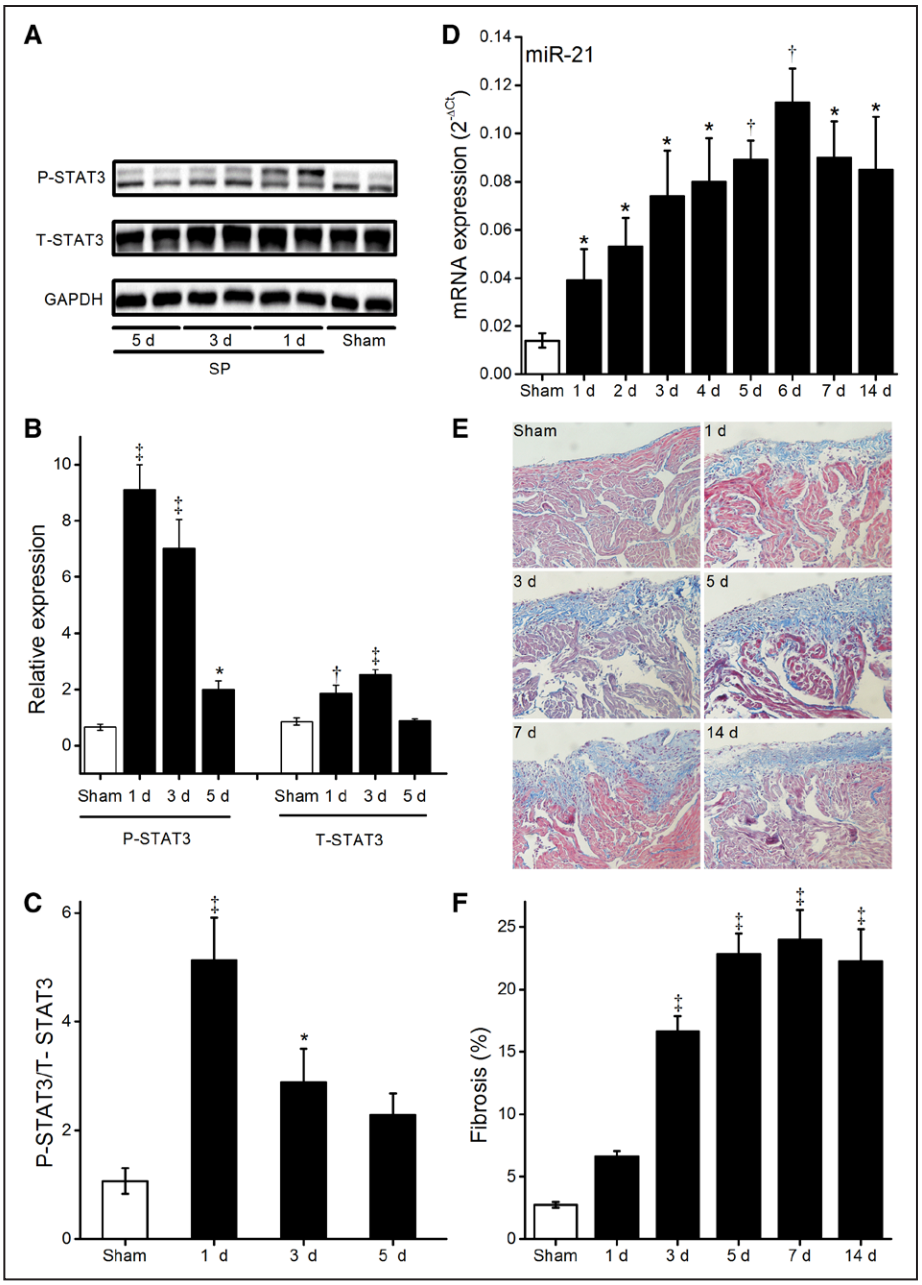


**Figure 2.** Representative Western blots for total and Tyr$^{705}$-phosphorylated signal transducer and activator of transcription 3 (STAT3; **A**), quantification of total and phosphorylated STAT3 relative to GAPDH (**B**), and the ratio of P-STAT3/T-STAT3 (**C**) from sham (n=5) and sterile pericarditis (SP) rats 1 d (n=4), 3 d (n=4), and 5 d (n=3) after surgery. **D**, The mRNA expression of miR-21 in atria from sham (n=5) and SP rats during postoperative days 1 to 14 (n=4 for each group). Representative histological sections stained with Masson trichrome (**E**) and percentage of left atrial interstitial fibrosis (**F**) from Sham and SP rats at 1 d (n=5), 3 d (n=4), 5 d (n=4), 7 d (n=3), and 14 d (n=4) after surgery. Original magnification ×400. *$P$<0.05, †$P$<0.01, ‡$P$<0.001 vs sham.

The atrial conduction velocity and index of inhomogeneity calculated from the isochrone map are shown in Table 1. The index of inhomogeneity was significantly greater in SP rats than in sham animals, but no difference was found in the conduction velocity (Table 1).

## Expression of STAT3 and miR-21 in SP Rats

Several studies have shown that the action of proinflammatory cytokines, particularly IL-6, on STAT3 can positively regulate miR-21 transcription.[28–30,39] The combination of STAT3/miR-21 has been implicated in amplifying the fibrogenic process. Thus, we measured the time-dependent changes in the expression levels of STAT3 and miR-21 in the atria after surgery. Western blot analysis (Figure 2A–2C ; Figure II in the Data Supplement) was applied to examine the protein level of T-STAT3 and P-STAT3, and real-time PCR (Figure 2D) was used to measure the miR-21 expression. The maximum P-STAT3 expression was observed on day 1 after surgery, when miR-21 expression began to increase, and remained present at high levels after day 5

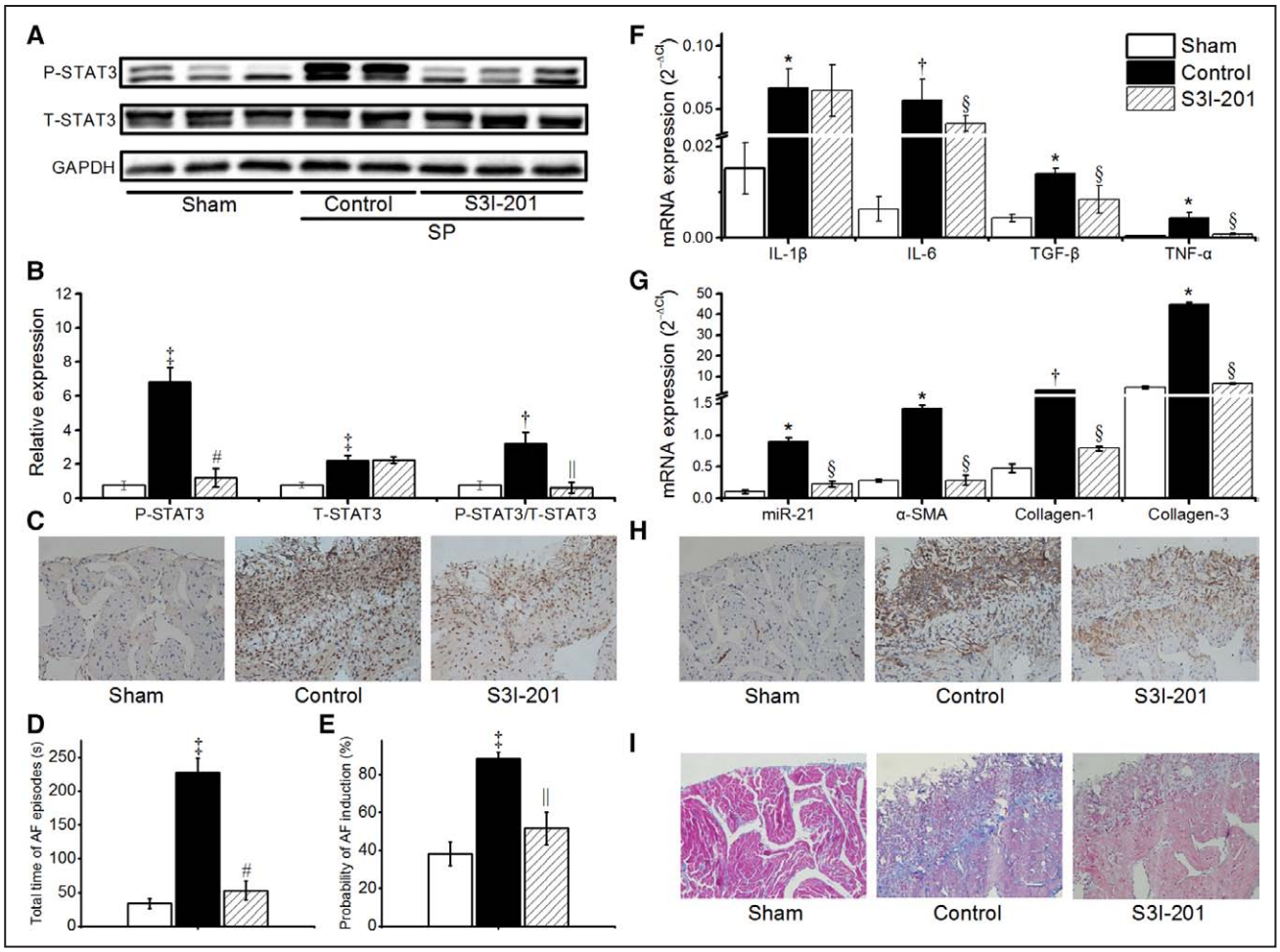


**Figure 3.** Results from sterile pericarditis (SP) rats treated with S3I-201 (n=5 for each group). Original Western blot (**A**) and quantification of total and phosphorylated signal transducer and activator of transcription 3 (STAT3) and the ratio of P-STAT3/T-STAT3 (**B**) in rats 3 days after surgery. **C**, Examples of phosphorylated STAT3 immunohistochemical staining. Total time of atrial fibrillation (AF) episodes (**D**) and probability of induced AF (**E**). **F**, The mRNA expression of interleukin (IL)-1β, IL-6, transforming growth factor (TGF)-β, and tumor necrosis factor (TNF)-α by real-time polymerase chain reaction (PCR). **G**, The mRNA expression of miR-21, α-SMA, collagen-1, and collagen-3 by real-time PCR. **H**, Examples of α-smooth muscle actin (α-SMA) immunohistochemical staining. **I**, Representative histological sections stained with Masson trichrome. **P*<0.05, †*P*<0.01, ‡*P*<0.001 vs sham; §*P*<0.05, ‖*P*<0.01, #*P*<0.001 vs control.

(Figure 2D), when the atria showed more extensive interstitial fibrosis in SP rats (Figure 2E and 2F). T-STAT3 also increased but to a lesser extent than P-STAT3 (Figure 2B). The other pathways, such as Spry-1/Erk-Mark[20] and the endothelial-to-mesenchymal transition,[40] did not play important roles in the fibrosis of SP rats (Figure III in the Data Supplement).

## STAT3 Inhibitor S3I-201 Reduced AF Vulnerability, Decreased miR-21 Expression, and Suppressed Fibrosis in SP Rats

To further investigate the role of STAT3 in POAF, we treated the SP rats with the STAT3 inhibitor S3I-201 (at 5 mg/kg) 5 minutes before surgery. As shown in Figure 3A and 3B and Figure IV in the Data Supplement, the administration of S3I-201 largely suppressed P-STAT3 on day 3 after pericardiotomy without significant effects on T-STAT3 expression. Immunohistochemical staining also showed a significant decrease in P-STAT3 in rat atrial tissue after S3I-201 treatment (Figure 3C). Meanwhile, the total AF duration and the probability of AF induction were significantly lower in rats treated with S3I-201 than in rats treated with the vehicle (Figure 3D and 3E). S3I-201 administration reduced the SP-induced inhomogeneous conduction (Table 1). In addition, most AF-related cytokines, IL-6, transforming growth factor-β, and tumor necrosis factor-α (but not IL-1β), were significantly reduced by S3I-201 treatment (Figure 3F). Furthermore, the SP-induced mRNA expression of miR-21 was significantly decreased after S3I-201 treatment (Figure 3G). Notably, as shown in Figure 3I, treatment with S3I-201 markedly reduced the percentage of fibrosis area (11.22±1.06% versus 17.73±1.32%; n=5; *P*<0.001). Consistently, the mRNA expression of the fibrosis-related genes α-SMA, collagen-1, and collagen-3 decreased significantly after S3I-201 administration (Figure 3G). The results of α-SMA expression were confirmed by immunohistochemical staining (Figure 3H).

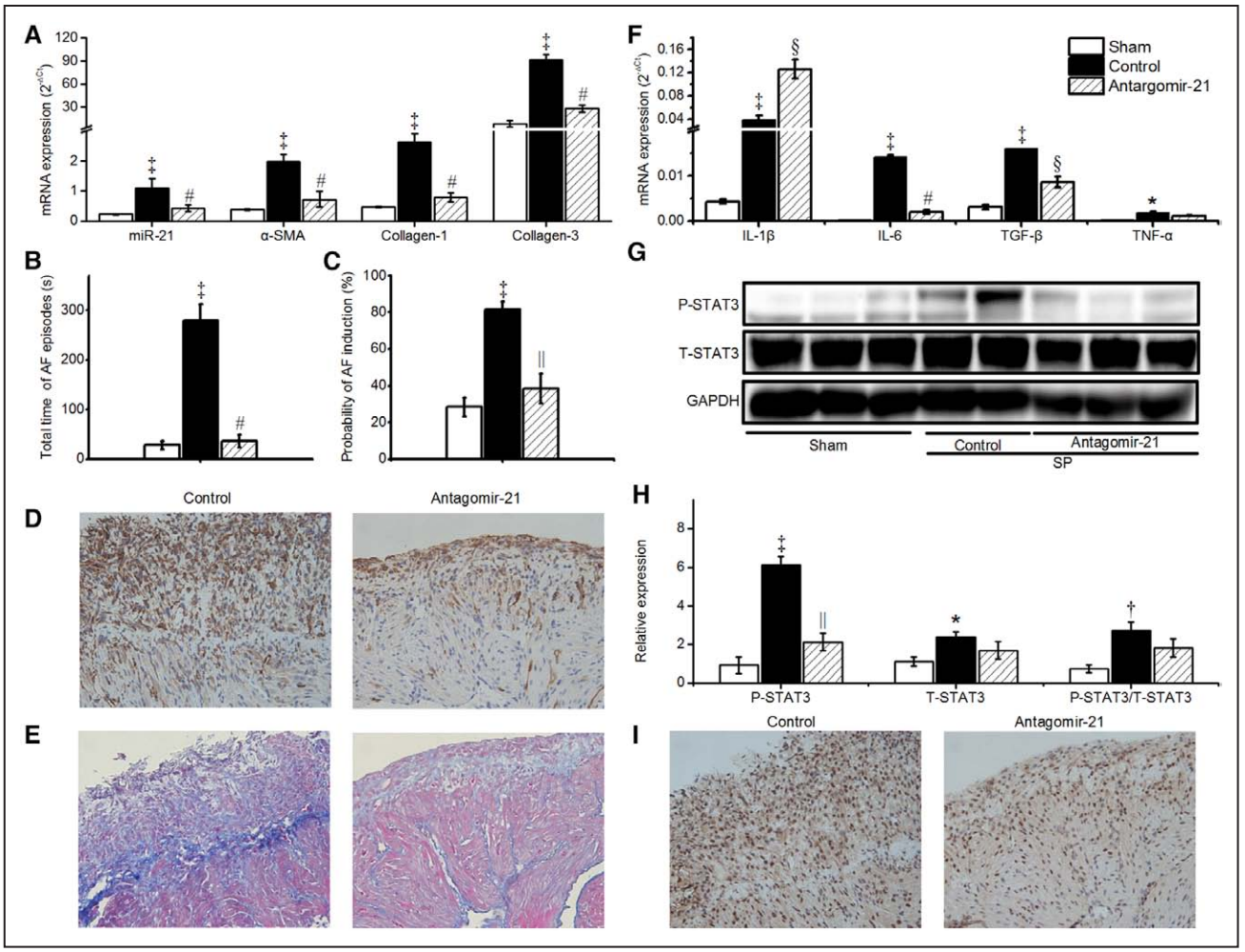


**Figure 4.** Results from sterile pericarditis (SP) rats treated with antagomir-21 (n=5, for each group). **A**, The mRNA expression levels of microRNA-21 (miR-21), α-smooth muscle actin (α-SMA), collagen-1, and collagen-3 in rats 3 days after surgery. Total time of atrial fibrillation (AF) episodes (**B**) and probability of induced AF (**C**). **D**, Examples of α-SMA immunohistochemical staining. **E**, Representative histological sections stained with Masson trichrome. **F**, The mRNA expression of interleukin (IL)-1β, IL-6, transforming growth factor (TGF)-β, and tumor necrosis factor (TNF)-α by real-time polymerase chain reaction (PCR). Original Western blot (**G**) and quantification of total and phosphorylated signal transducer and activator of transcription 3 (STAT3; **H**). **I**, Examples of phosphorylated STAT3 immunohistochemical staining. **P*<0.05, †*P*<0.01, ‡*P*<0.001 vs sham; §*P*<0.05, ‖*P*<0.01, #*P*<0.001 vs control.

## Treatment With Antagomir-21 Reduces AF Vulnerability, Suppresses Fibrosis, and Decreases STAT3 Phosphorylation in SP Rats

To further evaluate the role of miR-21 in POAF, we performed an experiment in which antagomir-21 was injected into the rat left atrial tissue during surgery. Atrial miR-21 expression was repressed on day 3 after surgery, as shown by real-time PCR (Figure 4A). Similarly to the effects of STAT3 inhibitor S3I-201 described above, treatment with antagomir-21 significantly prevented AF promotion (Figure 4B and 4C), alleviated atrial remodeling (Figure 4A, 4D, and 4E), and abrogated inhomogeneous conduction (Table 1) in SP rats. The percentage of fibrosis area was reduced from 17.88±1.28% to 13.02±0.98% (*P*<0.01; n=5). The SP-induced expression of proinflammatory cytokines, namely IL-6, transforming growth factor-β, and tumor necrosis factor-α, was significantly decreased by treatment with antagomir-21, but IL-1β was increased (Figure 4F). Importantly, P-STAT3 was also significantly inhibited (Figure 4G, 4H, and 4I; Figure V in the Data Supplement).

## STAT3 and miR-21 Expression Levels Are Upregulated During CF Activation

CF activation is critical in cardiac fibrosis. To confirm the STAT3 and miR-21 changes during CF activation, quiescent neonatal CFs were harvested and stimulated with recombinant IL-6 (20 ng/mL), which mimics the in vivo activation process. The culturing of neonatal CFs with recombinant IL-6 resulted in a rapid and transient increase in P-STAT3 levels, with a maximal STAT3 activation after 5 to 10 minutes (Figure 5B), confirming previous reports.[15] In contrast, miR-21 mRNA was augmented progressively over 24 to 48 hours (Figure 5D). Parallel incubation with IL-6 induced CFs proliferation (Figure 5E) and the mRNA expression of α-SMA, collagen-1, and collagen-3 in a time-dependent manner (Figure 5F). Similarly, we observed the robust activation of STAT3 (Figure 5A and 5C ; Figure VI in the Data Supplement) and the upregulation of miR-21 in addition to α-SMA, collagen-1, and collagen-3 upregulation in adult CFs stimulated with IL-6 (Figure 5G). Collectively, our results suggested that STAT3 and miR-21 might be involved in CF activation.

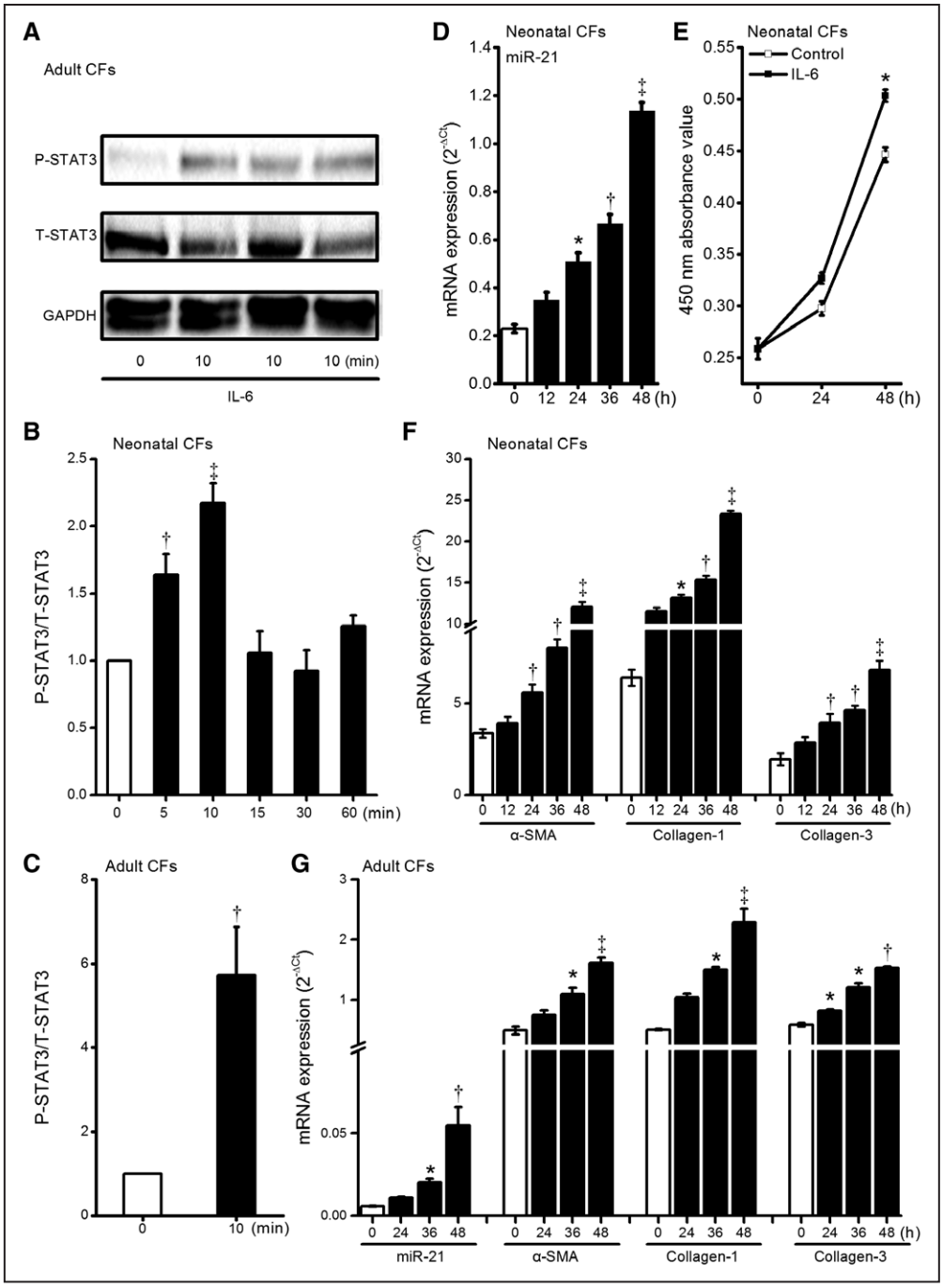


**Figure 5.** Interleukin (IL)-6–induced phosphorylation of signal transducer and activator of transcription 3 (STAT3) and microRNA-21 (miR-21) expression in cultured cardiac fibroblasts (CFs). CFs were stimulated with 20 ng/mL IL-6 for the indicated time periods. **A**, Phosphorylated and total STAT3 were analyzed by Western blotting in adult CFs. **B** and **C**, Quantification of total and phosphorylated STAT3 in neonatal (n=6) and adult CFs (n=5), respectively. The density of P-STAT3 was first normalized with respect to the density of T-STAT3, and the value after IL-6 stimulation was then normalized with respect to the basal value. **D**, Relative expression of microRNA-21 (miR-21) was examined by real-time polymerase chain reaction (PCR) in neonatal CFs (n=6). **E**, Cell numbers were detected using Cell Counting Kit-8, and the absorbance of the supernatant at 450 nm was measured spectrophotometrically in neonatal CFs (n=6). **F**, Relative expression levels of α-smooth muscle actin (α-SMA), collagen-1, and collagen-3 examined by real-time PCR in neonatal CFs (n=6). **G**, Relative expression levels of miR-21, α-SMA, collagen-1, and collagen-3 examined by real-time PCR in adult CFs (n=5). **P*<0.05, †*P*<0.01, ‡*P*<0.001 vs basal values.

## STAT3 Inhibitor S3I-201 Decreased IL-6–Induced miR-21 Expression and CF Activation

To confirm the role of STAT3 in IL-6–induced miR-21 expression and CF activation, we pretreated cultured neonatal CFs with the STAT3 inhibitor S3I-201 2 hours before IL-6 (20 ng/mL) stimulation. Figure 6A and Figure VII in the Data Supplement show that S3I-201 significantly inhibited P-STAT3 in both the absence and presence of IL-6 stimulation. As expected, S3I-201 blocked the IL-6–induced expression of miR-21, α-SMA, collagen-1, and collagen-3 (Figure 6B) in addition to CF proliferation

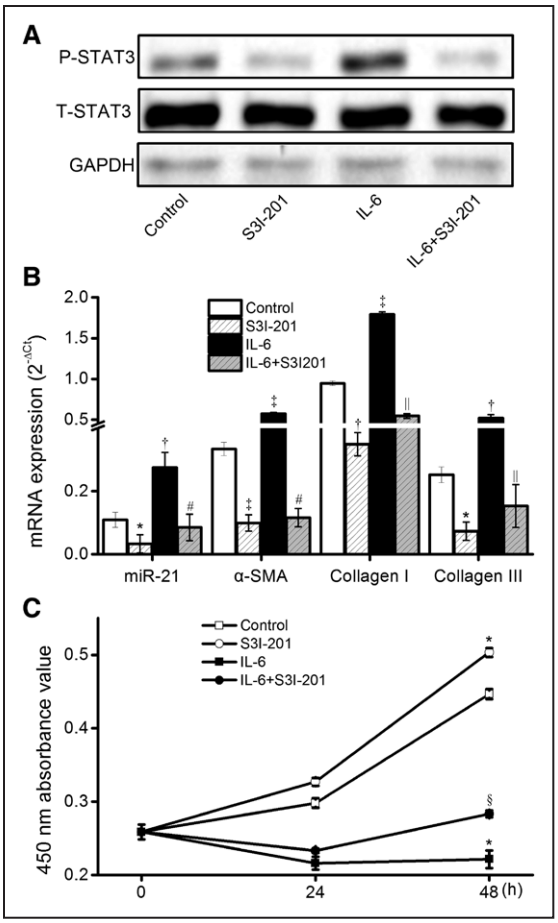


**Figure 6.** Effects of S3I-201 on phosphorylation of signal transducer and activator of transcription 3 (STAT3) and microRNA-21 (miR-21) and on cardiac fibroblast (CF) activation in the absence and presence of interleukin (IL)-6. CFs were preincubated with or without S3I-201 (50 or 100 nmol/L) for 30 minutes and stimulated with or without 20 ng/mL IL-6. **A**, Phosphorylated and total STAT3 were analyzed by western blotting. **B**, Relative expression levels of miR-21, α-smooth muscle actin (α-SMA), collagen-1, and collagen-3 were examined by real-time polymerase chain reaction (n=7). **C**, Cell numbers were detected using Cell Counting Kit-8, and the absorbance of the supernatant at 450 nm was measured spectrophotometrically (n=5). **P*<0.05, †*P*<0.01, ‡*P*<0.001 vs control; §*P*<0.05, ‖*P*<0.01, #*P*<0.001 vs IL-6.

(Figure 6C). We also observed reductions in the basal expression of miR-21, α-SMA, collagen-1, and collagen-3 and decreased cell numbers in CF cultures treated with 50 μmol/L S3I-201 (Figure 6B and 6C). Similar results were also obtained for adult CFs (data not shown).

### Antagomir-21 Decreases IL-6–Induced CF Activation and STAT3 Phosphorylation

To test the role of miR-21 in IL-6–induced CF activation and STAT3 phosphorylation, we transiently transfected antagomir-21 into neonatal CFs, followed by treatment with IL-6. Real-time PCR showed that miR-21 expression was significantly decreased after transfection with antagomir-21 (Figure 7A) compared with untransfected control cells. There was no difference between untransfected control cells and cells transfected with a negative control oligonucleotide. At the same time, the IL-6–induced expression of miR-21, α-SMA, collagen-1, and collagen-3 was completely blocked compared with the negative control (Figure 7A). After 48 hours, transfection with antagomir-21 resulted in decreased cell numbers in either the absence or presence of IL-6 stimulation compared with the negative control (Figure 7B). In addition, similarly to the effects of S3I-201, the knockdown of miR-21 in neonatal CFs significantly blocked STAT3 phosphorylation, which was also confirmed in adult CFs (Figure 7C and 7D; Figure VIII in the Data Supplement).

### Effect of miR-21 Overexpression on CF Activation and STAT3 Phosphorylation

To determine whether miR-21 would mimic IL-6–induced CF activation and STAT3 phosphorylation, mimic-miR-21 was transfected into neonatal CFs. The overexpression of miR-21 in the CFs enhanced the expression of miR-21, α-SMA, collagen-1, and collagen-3 (Figure 8A); increased the cell numbers (Figure 8B); and caused the upregulation of P-STAT3 (Figure 8C; Figure IX in the Data Supplement). The upregulation of P-STAT3 was also observed in adult CFs overexpressing miR-21 (Figure 8D). These results suggested that miR-21 also played a direct role in fibrogenesis and promoted STAT3 phosphorylation in CFs.

## Discussion

### Major Findings

In this study, we have uncovered a novel reciprocal loop between STAT3 and miR-21 that is activated after heart surgery and can contribute to AF by promoting atrial fibrosis. We observed the upregulation of STAT3 and miR-21 in a model of atrial profibrillatory remodeling in SP rats. The inhibition of STAT3 by S3I-201 resulted in the downregulation of miR-21, which ameliorated atrial fibrosis and attenuated the inducibility and maintenance of AF in SP rats. Similarly, the knockdown of miR-21 with antagomir-21 decreased the activation of STAT3, ameliorated atrial fibrosis, and prevented inducible AF in SP rats. In cultured CFs, IL-6 induced STAT3 phosphorylation, miR-21 expression, and CF activation, which were inhibited by S3I-201 and antagomir-21. In addition, miR-21 overexpression resulted in CF activation with higher levels of STAT3 phosphorylation. Our study may provide new insights into the pathophysiology of atrial fibrosis and innovative therapies for POAF.

### STAT3, miR-21, POAF, and Atrial Fibrosis

Atrial fibrosis, which can be activated by inflammation pathways, plays an important role in the initiation and maintenance of AF. Biopsies and autopsies from patients and animal models with AF have displayed the presence of atrial fibrosis.[41] There exist, however, controversial opinions regarding whether structural changes in the atria contribute to POAF.[42,43] In this study, we observed that SP rats exhibited a significantly increased incidence of inducible AF, extensive fibrosis, and high upregulation of genes encoding fibrogenic factors (α-SMA, collagen-1, and collagen-3) and proinflammatory cytokines (IL-1β, IL-6, transforming growth factor-β, and tumor necrosis factor-α). Although conduction velocity values in the

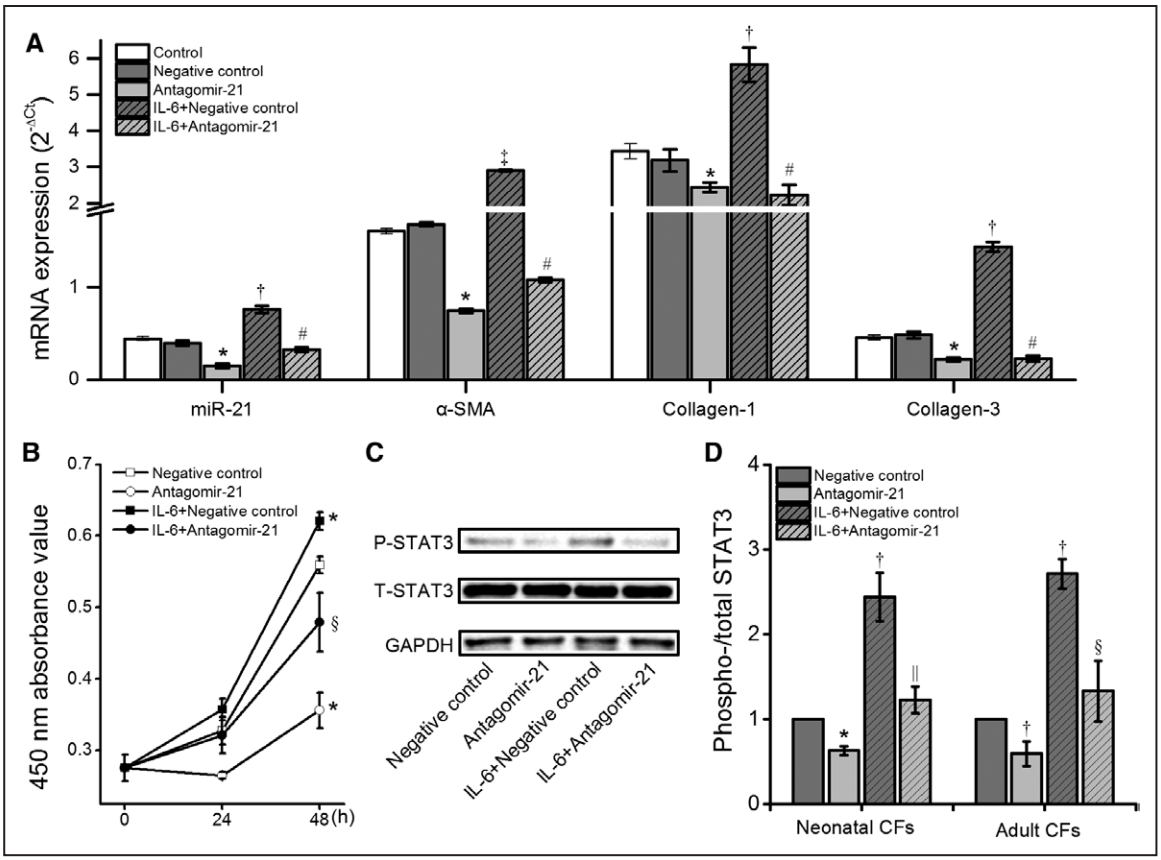


**Figure 7.** Effects of antagomir-21 on microRNA-21 (miR-21), cardiac fibroblast (CF), activation and phosphorylation of STAT3 in the absence and presence of interleukin (IL-6). CFs were transfected with antagomir-21 or negative control oligonucleotide and stimulated with or without 20 ng/mL IL-6. **A**, Relative expression of miR-21, α-SMA, collagen-1, and collagen-3 examined by real-time PCR in neonatal CFs (n=7). **B**, Cell numbers were detected using Cell Counting Kit-8, and absorbance of the supernatant at 450 nm was measured spectrophotometrically in neonatal CFs (n=4). **C** and **D**, Phosphorylated and total signal transducer and activator of transcription 3 (STAT3) were analyzed by Western blotting in neonatal (n=6) or adult CFs (n=4). **P*<0.05, †*P*<0.01, ‡*P*<0.001 vs negative control; §*P*<0.05, ‖*P*<0.01, #*P*<0.001 vs IL-6+negative control.

right atrium were similar across the groups, the index of inhomogeneity was increased by SP. These findings are consistent with previous studies in a canine SP model,[44,45] suggesting that atrial fibrosis may disturb atrial conduction and contribute to the increased vulnerability to AF in the SP model.

The abnormal expression of STAT3 and miR-21 has been found to promote atrial fibrosis.[17,25] In this study, we observed higher expression levels of T-STAT3, P-STAT3, and miR-21 in SP rats than in sham rats. The inhibition of STAT3 (SI-301) or knockdown of miR-21 (antagomir-21) ameliorated atrial fibrosis, reduced inhomogeneous conduction, and prevented inducible AF in SP rats. We also found increased expression levels of P-STAT3 and miR-21 in cultured CFs in response to IL-6, a known activator of fibrosis, associated with increased cell numbers and enhanced expression levels of α-SMA, collagen-1, and collagen-3. Moreover, IL-6–induced CF activation was completely abolished by S3I-201 and antagomir-21. Notably, transfected antagomir-21 also inhibited the basal expression of fibrosis-related genes, indicating that miR-21 plays a direct fibrogenic role in normal unstimulated rat CFs; however, the mechanisms require further study. Similar observations were made in the previous report.[46] The overexpression of miR-21 also caused CF activation. Taken together, our data demonstrated that STAT3 and miR-21 could contribute to AF by promoting atrial fibrosis in SP rats.

S3I-201, a cell-permeable amidosalicylic acid compound, showed selective blocking of STAT3 DNA binding and gene expression.[18] In vitro, S3I-201 inhibited the proliferation and survival of cancer cells. In vivo, the administration of S3I-201 (at 5 mg/kg) inhibited tumor growth in xenograft models. Subsequent investigation by other researchers demonstrated that S3I-201 also exhibits antifibrosis activity.[19] All these preclinical studies demonstrated that S3I-201 was well tolerated and exhibited no toxicity. Clinical trials of other STAT3 inhibitors showed that the most frequently reported treatment-related adverse events were gastrointestinal and were primarily of grade 1/2.[47]

STAT3 has been shown to bind to multiple sites in the miR-21 promoter and to directly activate the transcription of miR-21 on stimulation with IL-6 in many cell types.[28] Here, we found that the inactivation of STAT3 by S3I-201 significantly decreased the expression of miR-21 in cultured CFs stimulated with IL-6 and in the atria of SP rats. Considering the role of STAT3 in atrial fibrosis, as discussed above, our results suggested that STAT3 could act as an upstream regulator of miR-21 in CFs, promoting atrial fibrosis through the targets of miR-21 in SP rats.

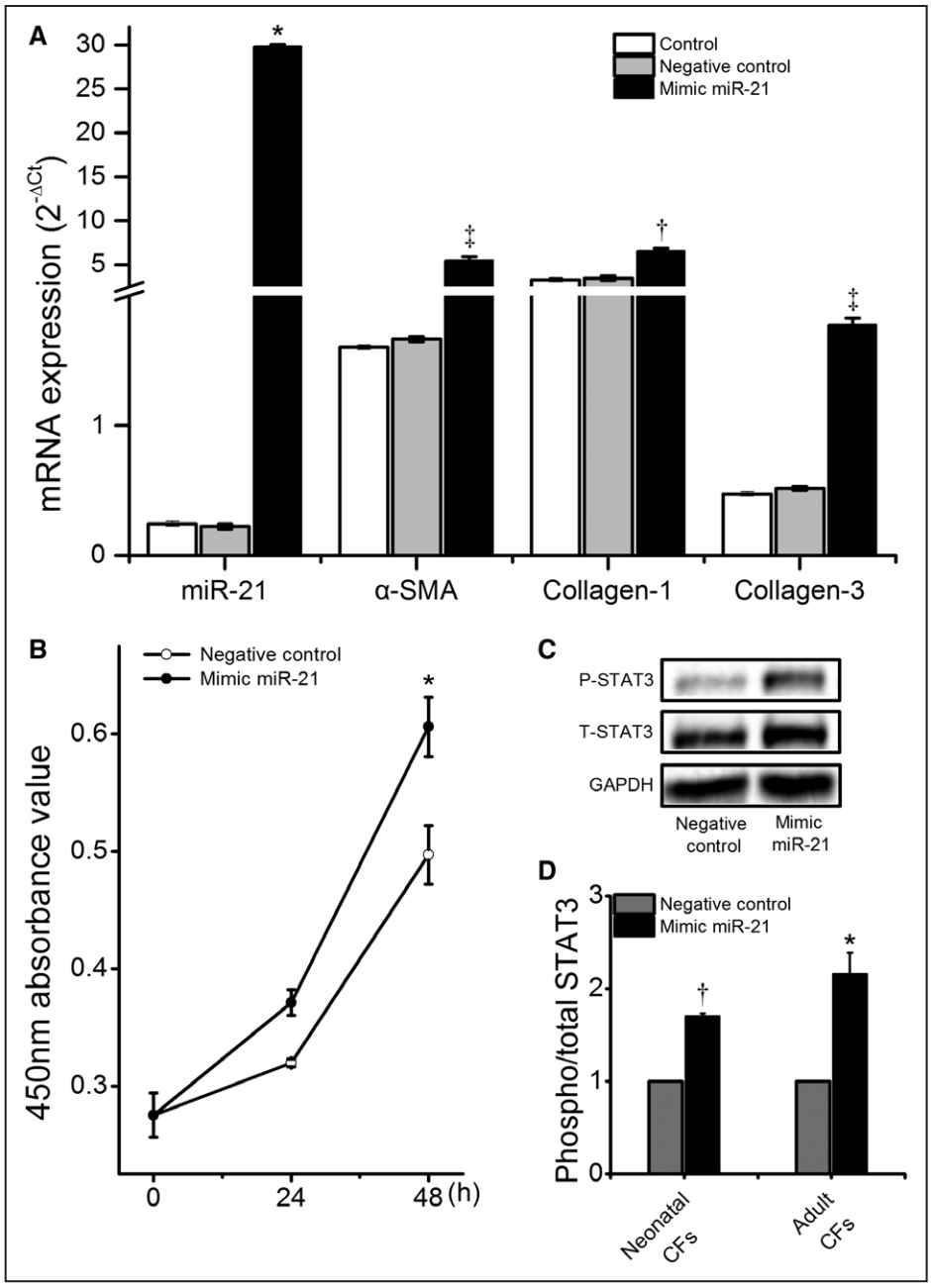


**Figure 8.** Effects of overexpression of microRNA-21 (miR-21) on cardiac fibroblast (CF) activation and signal transducer and activator of transcription 3 (STAT3) phosphorylation. CFs were transfected with mimic miR-21 or negative control oligonucleotide. **A**, Relative expression levels of miR-21, α-smooth muscle actin (α-SMA), collagen-1, and collagen-3 were examined by real-time PCR in neonatal CFs (n=6). **B**, Cell numbers were detected using Cell Counting Kit-8, and the absorbance of the supernatant at 450 nm was measured spectrophotometrically in neonatal CFs (n=6). **C** and **D**, Phosphorylated and total STAT3 were analyzed by Western blotting in neonatal (n=6) or adult CFs (n=4). **P*<0.05, †*P*<0.01, ‡*P*<0.001 vs negative control.

Conversely, miR-21 also regulates STAT3 in malignant disease.[39,48] Thus, we evaluated the expression of P-STAT3 in cultured CFs transfected with antagomir-21, miR-21 mimics, and a negative control. The reduction or enhancement of miR-21 levels was confirmed by real-time PCR. The data showed that antagomir-21 inhibited the activation of STAT3 in the absence or presence of IL-6, whereas miR-21 mimics caused a proportional increase in P-STAT3. Our data from SP rats also suggested that miR-21 enhanced the STAT3 activity. Previous studies demonstrated that miR-21 enhanced STAT3 signaling by directly inhibiting the protein inhibitor of activated STAT3 (PIAS3) in U266 myeloma cells[49] and MCF-7 breast cancer cells.[33] PIAS3 is a known negative regulator of the STAT3 pathway.[50] Thus, miR-21 might also indirectly upregulate STAT3 by inhibiting PIAS3 in CFs, which will require further detailed investigation.

## Study Limitations

This study was subject to certain limitations. Like all animal models of human disease, the model we used here is not a

perfect counterpart of any human condition. Further human studies are needed to verify our results. In this study, we only assessed the roles of STAT3 and miR-21 in atrial fibrosis; additional studies focusing on electric remodeling and the mechanisms of the STAT3/miR-21 feedback loop are also warranted.

### Conclusions

In summary, we have clearly shown that atrial fibrosis and AF promotion in SP rats are associated with STAT3 and miR-21. The inhibition of STAT3 or miR-21 ameliorated atrial fibrosis and prevented inducible AF in SP rats. More importantly, treatment with S3I-201 significantly decreased miR-21 expression. Meanwhile, the inhibition of miR-21 also decreased the activation of STAT3. The positive reciprocal loop between STAT3 and miR-21 and their roles in cardiac fibrosis were also confirmed in vitro using rat CFs. Our results suggested that the STAT3/miR-21 positive feedback loop might contribute to AF by promoting atrial fibrosis in SP rats.

## Appendix

From the Department of Cardiology, The First Affiliated Hospital of Xiamen University, Xiamen, China (Z.H., W.-h.L., Q.X.); Department of Cardiology, Quanzhou Hospital of Traditional Chinese Medicine, Quanzhou, China (X.-j.C.); and Research Center of Ion Channelopathy, Institute of Cardiology (C.Q., Q.D., D.D., Q.-f.W., J.L., X.C., N.Z., Y.-m.D., Y.-h.L.) and Department of Cardiovascular Surgery (H.-f.W.), Union Hospital, Tongji Medical College, Huazhong University of Science and Technology, Wuhan, P. R. China.

## Acknowledgments

We thank Drs Anruo Zou and Guoliang Hao for their excellent assistance in the use of epicardial activation mapping.

## Sources of Funding

This work was supported by grants from the National Nature Science Foundation of China to Dr Du (No. 81170164 and No. 81470421) and to Dr Huang (No. 81170090) and from the National Basic Research Program of China to Dr Cheng (973 Program: 2013CB531103).

## Disclosures

None.

## References

1. Yadava M, Hughey AB, Crawford TC. Postoperative atrial fibrillation: incidence, mechanisms, and clinical correlates. *Cardiol Clin*. 2014;32:627–636. doi: 10.1016/j.ccl.2014.07.002.
2. Ucar HI, Tok M, Atalar E, Dogan OF, Oc M, Farsak B, Guvener M, Yilmaz M, Dogan R, Demircin M, Pasaoglu I. Predictive significance of plasma levels of interleukin-6 and high-sensitivity C-reactive protein in atrial fibrillation after coronary artery bypass surgery. *Heart Surg Forum*. 2007;10:E131–E135. doi: 10.1532/HSF98.20061175.
3. Jacob KA, Nathoe HM, Dieleman JM, van Osch D, Kluin J, van Dijk D. Inflammation in new-onset atrial fibrillation after cardiac surgery: a systematic review. *Eur J Clin Invest*. 2014;44:402–428. doi: 10.1111/eci.12237.
4. Pagé PL, Plumb VJ, Okumura K, Waldo AL. A new animal model of atrial flutter. *J Am Coll Cardiol*. 1986;8:872–879.
5. Zhang Z, Zhang C, Wang H, Zhao J, Liu L, Lee J, He Y, Zheng Q. n-3 polyunsaturated fatty acids prevents atrial fibrillation by inhibiting inflammation in a canine sterile pericarditis model. *Int J Cardiol*. 2011;153:14–20. doi: 10.1016/j.ijcard.2010.08.024.
6. Ishii Y, Schuessler RB, Gaynor SL, Yamada K, Fu AS, Boineau JP, Damiano RJ Jr. Inflammation of atrium after cardiac surgery is associated with inhomogeneity of atrial conduction and atrial fibrillation. *Circulation*. 2005;111:2881–2888. doi: 10.1161/CIRCULATIONAHA.104.475194.
7. Meléndez GC, McLarty JL, Levick SP, Du Y, Janicki JS, Brower GL. Interleukin 6 mediates myocardial fibrosis, concentric hypertrophy, and diastolic dysfunction in rats. *Hypertension*. 2010;56:225–231. doi: 10.1161/HYPERTENSIONAHA.109.148635.
8. Diaz JA, Booth AJ, Lu G, Wood SC, Pinsky DJ, Bishop DK. Critical role for IL-6 in hypertrophy and fibrosis in chronic cardiac allograft rejection. *Am J Transplant*. 2009;9:1773–1783. doi: 10.1111/j.1600-6143.2009.02706.x.
9. Gaudino M, Andreotti F, Zamparelli R, Di Castelnuovo A, Nasso G, Burzotta F, Iacoviello L, Donati MB, Schiavello R, Maseri A, Possati G. The -174G/C interleukin-6 polymorphism influences postoperative interleukin-6 levels and postoperative atrial fibrillation. Is atrial fibrillation an inflammatory complication? *Circulation*. 2003;108(suppl 1):I195–I199.
10. Hu YF, Chen YJ, Lin YJ, Chen SA. Inflammation and the pathogenesis of atrial fibrillation. *Nat Rev Cardiol*. 2015;12:230–243. doi: 10.1038/nrcardio.2015.2.
11. Maesen B, Nijs J, Maessen J, Allessie M, Schotten U. Post-operative atrial fibrillation: a maze of mechanisms. *Europace*. 2012;14:159–174. doi: 10.1093/europace/eur208.
12. Levy DE, Darnell JE Jr. Stats: transcriptional control and biological impact. *Nat Rev Mol Cell Biol*. 2002;3:651–662. doi: 10.1038/nrm909.
13. Haghikia A, Ricke-Hoch M, Stapel B, Gorst I, Hilfiker-Kleiner D. STAT3, a key regulator of cell-to-cell communication in the heart. *Cardiovasc Res*. 2014;102:281–289. doi: 10.1093/cvr/cvu034.
14. Mihara M, Hashizume M, Yoshida H, Suzuki M, Shiina M. IL-6/IL-6 receptor system and its role in physiological and pathological conditions. *Clin Sci (Lond)*. 2012;122:143–159. doi: 10.1042/CS20110340.
15. Mir SA, Chatterjee A, Mitra A, Pathak K, Mahata SK, Sarkar S. Inhibition of signal transducer and activator of transcription 3 (STAT3) attenuates interleukin-6 (IL-6)-induced collagen synthesis and resultant hypertrophy in rat heart. *J Biol Chem*. 2012;287:2666–2677. doi: 10.1074/jbc.M111.246173.
16. Tsai CT, Lin JL, Lai LP, Lin CS, Huang SK. Membrane translocation of small GTPase Rac1 and activation of STAT1 and STAT3 in pacing-induced sustained atrial fibrillation. *Heart Rhythm*. 2008;5:1285–1293. doi: 10.1016/j.hrthm.2008.05.012.
17. Tsai CT, Lai LP, Kuo KT, Hwang JJ, Hsieh CS, Hsu KL, Tseng CD, Tseng YZ, Chiang FT, Lin JL. Angiotensin II activates signal transducer and activators of transcription 3 via Rac1 in atrial myocytes and fibroblasts: implication for the therapeutic effect of statin in atrial structural remodeling. *Circulation*. 2008;117:344–355. doi: 10.1161/CIRCULATIONAHA.107.695346.
18. Siddiquee K, Zhang S, Guida WC, Blaskovich MA, Greedy B, Lawrence HR, Yip ML, Jove R, McLaughlin MM, Lawrence NJ, Sebti SM, Turkson J. Selective chemical probe inhibitor of Stat3, identified through structure-based virtual screening, induces antitumor activity. *Proc Natl Acad Sci USA*. 2007;104:7391–7396. doi: 10.1073/pnas.0609757104.
19. Pang M, Ma L, Gong R, Tolbert E, Mao H, Ponnusamy M, Chin YE, Yan H, Dworkin LD, Zhuang S. A novel STAT3 inhibitor, S3I-201, attenuates renal interstitial fibroblast activation and interstitial fibrosis in obstructive nephropathy. *Kidney Int*. 2010;78:257–268. doi: 10.1038/ki.2010.154.
20. Thum T, Gross C, Fiedler J, Fischer T, Kissler S, Bussen M, Galuppo P, Just S, Rottbauer W, Frantz S, Castoldi M, Soutschek J, Koteliansky V, Rosenwald A, Basson MA, Licht JD, Pena JT, Rouhanifard SH, Muckenthaler MU, Tuschl T, Martin GR, Bauersachs J, Engelhardt S. MicroRNA-21 contributes to myocardial disease by stimulating MAP kinase signalling in fibroblasts. *Nature*. 2008;456:980–984. doi: 10.1038/nature07511.
21. Roy S, Khanna S, Hussain SR, Biswas S, Azad A, Rink C, Gnyawali S, Shilo S, Nuovo GJ, Sen CK. MicroRNA expression in response to murine myocardial infarction: miR-21 regulates fibroblast metalloprotease-2 via phosphatase and tensin homologue. *Cardiovasc Res*. 2009;82:21–29. doi: 10.1093/cvr/cvp015.
22. Patrick DM, Montgomery RL, Qi X, Obad S, Kauppinen S, Hill JA, van Rooij E, Olson EN. Stress-dependent cardiac remodeling occurs in the absence of microRNA-21 in mice. *J Clin Invest*. 2010;120:3912–3916. doi: 10.1172/JCI43604.
23. Villar AV, García R, Merino D, Llano M, Cobo M, Montalvo C, Martín-Durán R, Hurlé MA, Nistal JF. Myocardial and circulating levels of microRNA-21 reflect left ventricular fibrosis in aortic stenosis patients. *Int J Cardiol*. 2013;167:2875–2881. doi: 10.1016/j.ijcard.2012.07.021.
24. Barana A, Matamoros M, Dolz-Gaitón P, Pérez-Hernández M, Amorós I, Núñez M, Sacristán S, Pedraz Á, Pinto Á, Fernández-Avilés F, Tamargo J, Delpón E, Caballero R. Chronic atrial fibrillation increases microRNA-21

in human atrial myocytes decreasing L-type calcium current. *Circ Arrhythm Electrophysiol*. 2014;7:861–868. doi: 10.1161/CIRCEP.114.001709.
25. Adam O, Löhfelm B, Thum T, Gupta SK, Puhl SL, Schäfers HJ, Böhm M, Laufs U. Role of miR-21 in the pathogenesis of atrial fibrosis. *Basic Res Cardiol*. 2012;107:278. doi: 10.1007/s00395-012-0278-0.
26. Liu Z, Zhou C, Liu Y, Wang S, Ye P, Miao X, Xia J. The expression levels of plasma micoRNAs in atrial fibrillation patients. *PLoS One*. 2012;7:e44906. doi: 10.1371/journal.pone.0044906.
27. Cardin S, Guasch E, Luo X, Naud P, Le Quang K, Shi Y, Tardif JC, Comtois P, Nattel S. Role for microRNA-21 in atrial profibrillatory fibrotic remodeling associated with experimental postinfarction heart failure. *Circ Arrhythm Electrophysiol*. 2012;5:1027–1035. doi: 10.1161/CIRCEP.112.973214.
28. Löffler D, Brocke-Heidrich K, Pfeifer G, Stocsits C, Hackermüller J, Kretzschmar AK, Burger R, Gramatzki M, Blumert C, Bauer K, Cvijic H, Ullmann AK, Stadler PF, Horn F. Interleukin-6 dependent survival of multiple myeloma cells involves the Stat3-mediated induction of microRNA-21 through a highly conserved enhancer. *Blood*. 2007;110:1330–1333. doi: 10.1182/blood-2007-03-081133.
29. Iliopoulos D, Jaeger SA, Hirsch HA, Bulyk ML, Struhl K. STAT3 activation of miR-21 and miR-181b-1 via PTEN and CYLD are part of the epigenetic switch linking inflammation to cancer. *Mol Cell*. 2010;39:493–506. doi: 10.1016/j.molcel.2010.07.023.
30. van der Fits L, van Kester MS, Qin Y, Out-Luiting JJ, Smit F, Zoutman WH, Willemze R, Tensen CP, Vermeer MH. MicroRNA-21 expression in CD4+ T cells is regulated by STAT3 and is pathologically involved in Sézary syndrome. *J Invest Dermatol*. 2011;131:762–768. doi: 10.1038/jid.2010.349.
31. Ren Y, Zhou X, Mei M, Yuan XB, Han L, Wang GX, Jia ZF, Xu P, Pu PY, Kang CS. MicroRNA-21 inhibitor sensitizes human glioblastoma cells U251 (PTEN-mutant) and LN229 (PTEN-wild type) to taxol. *BMC Cancer*. 2010;10:27. doi: 10.1186/1471-2407-10-27.
32. Qian X, Ren Y, Shi Z, Long L, Pu P, Sheng J, Yuan X, Kang C. Sequence-dependent synergistic inhibition of human glioma cell lines by combined temozolomide and miR-21 inhibitor gene therapy. *Mol Pharm*. 2012;9:2636–2645. doi: 10.1021/mp3002039.
33. Wang Z, Han J, Cui Y, Zhou X, Fan K. miRNA-21 inhibition enhances RANTES and IP-10 release in MCF-7 via PIAS3 and STAT3 signalling and causes increased lymphocyte migration. *Biochem Biophys Res Commun*. 2013;439:384–389. doi: 10.1016/j.bbrc.2013.08.072.
34. Fu XX, Zhao N, Dong Q, Du LL, Chen XJ, Wu QF, Cheng X, Du YM, Liao YH. Interleukin-17A contributes to the development of post-operative atrial fibrillation by regulating inflammation and fibrosis in rats with sterile pericarditis. *Int J Mol Med*. 2015;36:83–92. doi: 10.3892/ijmm.2015.2204.
35. Davies L, Jin J, Shen W, Tsui H, Shi Y, Wang Y, Zhang Y, Hao G, Wu J, Chen S, Fraser JA, Dong N, Christoffels V, Ravens U, Huang CL, Zhang H, Cartwright EJ, Wang X, Lei M. Mkk4 is a negative regulator of the transforming growth factor beta 1 signaling associated with atrial remodeling and arrhythmogenesis with age. *J Am Heart Assoc*. 2014;3:e000340. doi: 10.1161/JAHA.113.000340.
36. Kim SJ, Choisy SC, Barman P, Zhang H, Hancox JC, Jones SA, James AF. Atrial remodeling and the substrate for atrial fibrillation in rat hearts with elevated afterload. *Circ Arrhythm Electrophysiol*. 2011;4:761–769. doi: 10.1161/CIRCEP.111.964783.
37. Lammers WJ, Schalij MJ, Kirchhof CJ, Allessie MA. Quantification of spatial inhomogeneity in conduction and initiation of reentrant atrial arrhythmias. *Am J Physiol*. 1990;259(4 pt 2):H1254–H1263.
38. Zhao N, Dong Q, Du LL, Fu XX, Du YM, Liao YH. Potent suppression of Kv1.3 potassium channel and IL-2 secretion by diphenyl phosphine oxide-1 in human T cells. *PLoS One*. 2013;8:e64629. doi: 10.1371/journal.pone.0064629.
39. Sawant DV, Wu H, Kaplan MH, Dent AL. The Bcl6 target gene microRNA-21 promotes Th2 differentiation by a T cell intrinsic pathway. *Mol Immunol*. 2013;54:435–442. doi: 10.1016/j.molimm.2013.01.006.
40. Zeisberg EM, Tarnavski O, Zeisberg M, Dorfman AL, McMullen JR, Gustafsson E, Chandraker A, Yuan X, Pu WT, Roberts AB, Neilson EG, Sayegh MH, Izumo S, Kalluri R. Endothelial-to-mesenchymal transition contributes to cardiac fibrosis. *Nat Med*. 2007;13:952–961. doi: 10.1038/nm1613.
41. Jalife J, Kaur K. Atrial remodeling, fibrosis, and atrial fibrillation. *Trends Cardiovasc Med*. 2015;25:475–484. doi: 10.1016/j.tcm.2014.12.015.
42. Cosgrave J, Foley JB, Flavin R, O'briain DS, Fitzpatrick E, Bennett K, Young V, Tolan M, McGovern E. Preoperative atrial histological changes are not associated with postoperative atrial fibrillation. *Cardiovasc Pathol*. 2006;15:213–217. doi: 10.1016/j.carpath.2006.04.002.
43. Swartz MF, Fink GW, Lutz CJ, Taffet SM, Berenfeld O, Vikstrom KL, Kasprowicz K, Bhatta L, Puskas F, Kalifa J, Jalife J. Left versus right atrial difference in dominant frequency, K(+) channel transcripts, and fibrosis in patients developing atrial fibrillation after cardiac surgery. *Heart Rhythm*. 2009;6:1415–1422. doi: 10.1016/j.hrthm.2009.06.018.
44. Kumagai K, Nakashima H, Saku K. The HMG-CoA reductase inhibitor atorvastatin prevents atrial fibrillation by inhibiting inflammation in a canine sterile pericarditis model. *Cardiovasc Res*. 2004;62:105–111. doi: 10.1016/j.cardiores.2004.01.018.
45. Ryu K, Li L, Khrestian CM, Matsumoto N, Sahadevan J, Ruehr ML, Van Wagoner DR, Efimov IR, Waldo AL. Effects of sterile pericarditis on connexins 40 and 43 in the atria: correlation with abnormal conduction and atrial arrhythmias. *Am J Physiol Heart Circ Physiol*. 2007;293:H1231–H1241. doi: 10.1152/ajpheart.00607.2006.
46. Wei J, Feng L, Li Z, Xu G, Fan X. MicroRNA-21 activates hepatic stellate cells via PTEN/Akt signaling. *Biomed Pharmacother*. 2013;67:387–392. doi: 10.1016/j.biopha.2013.03.014.
47. Bendell JC, Hong DS, Burris HA 3rd, Naing A, Jones SF, Falchook G, Bricmont P, Elekes A, Rock EP, Kurzrock R. Phase 1, open-label, dose-escalation, and pharmacokinetic study of STAT3 inhibitor OPB-31121 in subjects with advanced solid tumors. *Cancer Chemother Pharmacol*. 2014;74:125–130. doi: 10.1007/s00280-014-2480-2.
48. Cao Q, Li YY, He WF, Zhang ZZ, Zhou Q, Liu X, Shen Y, Huang TT. Interplay between microRNAs and the STAT3 signaling pathway in human cancers. *Physiol Genomics*. 2013;45:1206–1214. doi: 10.1152/physiolgenomics.00122.2013.
49. Xiong Q, Zhong Q, Zhang J, Yang M, Li C, Zheng P, Bi LJ, Ge F. Identification of novel miR-21 target proteins in multiple myeloma cells by quantitative proteomics. *J Proteome Res*. 2012;11:2078–2090. doi: 10.1021/pr201079y.
50. Dabir S, Kluge A, Dowlati A. The association and nuclear translocation of the PIAS3-STAT3 complex is ligand and time dependent. *Mol Cancer Res*. 2009;7:1854–1860. doi: 10.1158/1541-7786.MCR-09-0313.